

Particular Topological Complexity of Lead Oxide Blocks in $\text{Pb}_{31}\text{O}_{22}\text{X}_{18}$
(X = Br, Cl)

Sergey V. Krivovichev,*† Oleg I. Siidra,† Evgenii V. Nazarchuk,† Peter C. Burns,‡ and Wulf Depmeier§

Department of Crystallography, St. Petersburg State University, University Emb. 7/9, 199034 St. Petersburg, Russia, Department of Civil Engineering and Geological Sciences, University of Notre Dame, 156 Fitzpatrick Hall, Notre Dame, Indiana 46556, and Institut für Geowissenschaften, Universität zu Kiel, Olshausenstrasse 40, 24118 Kiel, Germany

Received January 30, 2006

Dark-green platy crystals of the new compound $\text{Pb}_{31}\text{O}_{22}\text{Br}_{10}\text{Cl}_8$ (**1**) have been obtained by rapid quenching of a lead oxide halide melt. The structure of **1** (triclinic, $P\bar{1}$, $a = 12.1192(7)$ Å, $b = 16.2489(10)$ Å, $c = 18.3007(11)$ Å, $\alpha = 93.104(2)^\circ$, $\beta = 95.809(2)^\circ$, $\gamma = 111.252(1)^\circ$, $V = 3325.4(3)$ Å³, $Z = 2$) can be viewed as incorporation of $[\text{PbX}_6]^{4-}$ halide units (X = Br, Cl) into the defect PbO matrix. The latter represents a two-dimensional $[\text{O}_{22}\text{Pb}_{30}]^{16+}$ cationic layer of OPb_4 tetrahedra that can be derived from the $[\text{OPb}]$ tetrahedral layer observed in tetragonal PbO. The layer consists of 22 symmetrically inequivalent OPb_4 tetrahedra and represents the topologically most complicated arrangement of tetrahedra known to date.

Lead oxyhalides represent an important class of inorganic materials with possible applications as ionic conductors¹ and highly anisotropic nanomaterials.² They are also of great interest from the viewpoint of environmental chemistry³ and mineralogy.⁴ To date, detailed chemical and structural information is available for pure oxychloride,^{4a,f,5} oxybromide,⁶ and oxyiodide⁷ systems, whereas little is known about

mixed halide systems such as Cl–Br. However, these systems are of particular importance because of the presence of mixed lead oxychloride/oxybromide nanoparticles in atmospheric aerosols³ and the discovery of lead oxyhalide deposits on the pistons of failed aircraft engines.⁸ Here we report on the synthesis and structure of $\text{Pb}_{31}\text{O}_{22}\text{Br}_{10}\text{Cl}_8$ (**1**), a high-temperature phase in the $\text{PbO}\text{--}\text{PbCl}_2\text{--}\text{PbBr}_2$ system that has been obtained by rapid quenching of lead oxyhalide melt.

In a typical synthesis, 0.446 g (0.0020 mol) of PbO, 0.183 g (0.0005 mol) of PbBr_2 , and 0.140 g (0.0005 mol) of PbCl_2 were loaded into a platinum crucible and kept at 780 °C for 1 h in air, followed by cooling to 685 °C at a cooling rate of 9 °C/min. The mixture was kept at 685 °C for 15 min and then cooled to 675 °C at a cooling rate of 1 °C/min, followed by cooling to room temperature over 2.5 h. The product consisted of dark-green platy crystals of **1**. Powder diffraction patterns confirmed the presence of traces of another phase, which we were not able to identify. The chemical composition was established by semiquantitative electron microprobe analysis and crystal structure determination (see below). It is of interest that cooling of the same mixture down to room temperature at a lower cooling rate of a few degrees per hour results in the formation of transparent yellowish crystals of $\text{Pb}_3\text{O}_2(\text{Br},\text{Cl})_2$ with the structure of mendipite, $\text{Pb}_3\text{O}_2\text{Cl}_2$.^{4f,5} Thus, phase **1** is a metastable high-temperature phase that can be obtained exclusively by rapid quenching of the lead oxyhalide melt.

The structure of **1**⁹ is remarkable in many ways. It contains 31 symmetrically independent Pb^{2+} cations, 18 halide sites statistically occupied by Br^- and Cl^- ions, and 22 O positions. The Pb^{2+} cations of the $\text{Pb}1\text{--}\text{Pb}30$ sites have mixed oxyhalide coordination with $m\text{O} + n\text{X}$ anions (X = Br, Cl), where m and n range from 2 to 4 ($\text{Pb}\text{--}\text{O} = 2.16\text{--}2.58$ Å; $\text{Pb}\text{--}\text{X} = 2.78\text{--}3.55$ Å). Among the Pb atoms, the

* To whom correspondence should be addressed. E-mail: skrivovi@mail.ru.

† St. Petersburg State University.

‡ University of Notre Dame.

§ Universität zu Kiel.

- (1) Matsumoto, H.; Miyake, T.; Iwahara, H. *Mater. Res. Bull.* **2001**, *36*, 1177–1184.
- (2) Sigman, M. B., Jr.; Korgel, B. A. *J. Am. Chem. Soc.* **2005**, *127*, 10089–10095.
- (3) (a) Ter Haar, G. L.; Bayard, M. A. *Nature* **1971**, *232*, 553–554. (b) Post, J.; Buseck, P. R. *Environ. Sci. Technol.* **1985**, *19*, 682–685.
- (4) (a) Humphreys, D. A.; Thomas, J. H.; Williams, P. A.; Symes, R. F. *Mineral. Mag.* **1980**, *43*, 901–904. (b) Edwards, R.; Gillard, R. D.; Williams, P. A.; Pollard, A. M. *Mineral. Mag.* **1992**, *56*, 53–65. (c) Cooper, M. A.; Hawthorne, F. C. *Am. Mineral.* **1994**, *79*, 550–554. (d) Welch, M. D.; Criddle, A. J.; Symes, R. F. *Mineral. Mag.* **1998**, *62*, 387–393. (e) Welch, M. D.; Cooper, M. A.; Hawthorne, F. C.; Criddle, A. J. *Am. Mineral.* **2000**, *85*, 1526–1533. (f) Krivovichev, S. V.; Burns, P. C. *Eur. J. Mineral.* **2001**, *13*, 801–809. (g) Krivovichev, S. V.; Burns, P. C. *Eur. J. Mineral.* **2002**, *14*, 135–140. (h) Bonaccorsi, E.; Pasero, M. *Mineral. Mag.* **2003**, *67*, 15–21.
- (5) Vincent, H.; Perrault, G. *Bull. Soc. Fr. Mineral. Cristallogr.* **1971**, *94*, 323–331.

(6) (a) Keller, H. L. *Angew. Chem.* **1983**, *95*, 318–319. (b) Riebe, H.-J.; Keller, H. L. *Z. Anorg. Allg. Chem.* **1989**, *571*, 139–147.

(7) Kramer, V.; Post, E. *Mater. Res. Bull.* **1985**, *20*, 407–412.

(8) Noren, L.; Tan, E. S. Q.; Withers, R. L.; Sterns, M.; Rundlof, H. *Mater. Res. Bull.* **2002**, *37*, 1431–1442.

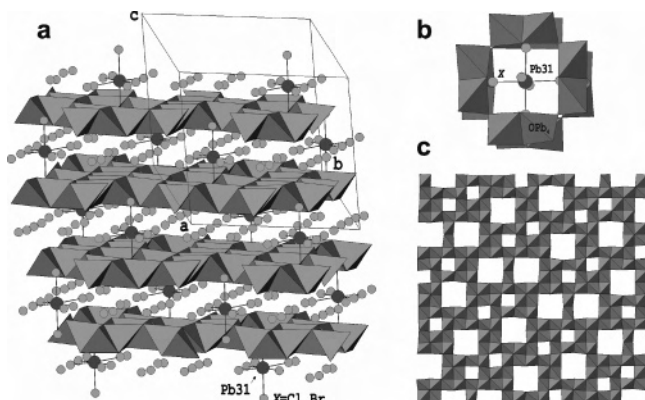


Figure 1. Crystal structure of $\text{Pb}_{31}\text{O}_{22}\text{X}_{18}$ (a), the $[\text{PbX}_6]^{4-}$ octahedral unit within the array of OPb_4 tetrahedra (b), and the $[\text{O}_{22}\text{Pb}_{30}]^{16+}$ 2D layer composed from edge-sharing OPb_4 tetrahedra (c).

Pb_5 , Pb_{12} , Pb_{21} , Pb_{23} – Pb_{25} , Pb_{28} , and Pb_{30} sites are coordinated by two O atoms ($m = 2$), the Pb_2 – Pb_4 , Pb_7 , Pb_9 , Pb_{11} , Pb_{13} , Pb_{15} , Pb_{17} – Pb_{20} , Pb_{22} , Pb_{26} , Pb_{27} , and Pb_{29} sites have $m = 3$, and the Pb_1 , Pb_6 , Pb_8 , Pb_{10} , Pb_{14} , and Pb_{16} sites have $m = 4$. The Pb_{31} site is coordinated solely by X anions, being at the center of $[\text{PbX}_6]^{4-}$ octahedral units [$\text{Pb}_{31}\text{--X} = 2.78\text{--}3.01 \text{ \AA}$]. All 22 O^{2-} anions are tetrahedrally coordinated by Pb^{2+} cations, thus forming oxocentered OPb_4 tetrahedra. It is notable that OPb_4 moieties are common in inorganic lead oxysalts^{4g,f,6,10} and have recently been recognized as important building blocks in tribasic lead maleate.¹¹

The structure of **1** (Figure 1a) can be described as incorporation of $[\text{PbX}_6]^{4-}$ halide units into a defect PbO matrix. The latter represents a two-dimensional (2D) $[\text{O}_{22}\text{Pb}_{30}]^{16+}$ cationic layer of the OPb_4 tetrahedra (Figure 1c) that can be derived from the $[\text{OPb}]$ tetrahedral layer that has been observed in tetragonal PbO .¹² To transform the $[\text{OPb}]$

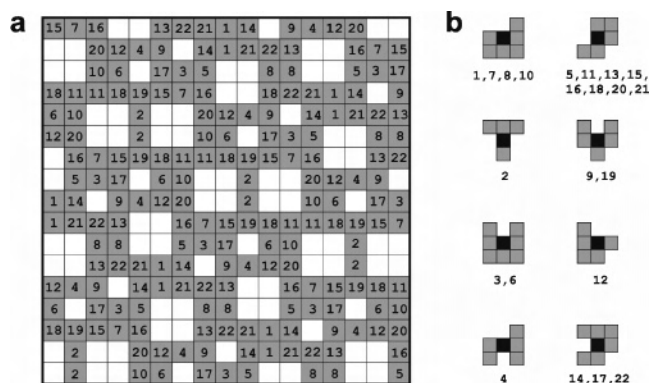


Figure 2. Topological structure of the $[\text{O}_{22}\text{Pb}_{30}]^{16+}$ 2D layer in the structure of **1** (a) and first coronas (local coordinations) of central OPb_4 tetrahedra (shown as black squares) (b). See the text for details.

layer into the $[\text{O}_{22}\text{Pb}_{30}]^{16+}$ layer observed in **1**, one has to excise certain blocks of OPb_4 tetrahedra from the former. This procedure is known for the PbO derivative structures¹⁰ⁿ and has been applied to rare-earth oxychalcogenides,¹³ sulfides,¹⁴ and intermetallic and cluster compounds¹⁵ as well. In the structure of **1**, holes in the 2D PbO matrix correspond to either single tetrahedra or 2×2 blocks. The $[\text{O}_{22}\text{Pb}_{30}]^{16+}$ cationic layers are parallel to the (102) plane and are separated by X^- anions, which form square pavements with X--X distances of $\sim 4 \text{ \AA}$. The $[\text{PbX}_6]^{4-}$ octahedra are located between the layers in such a way that membered 2×2 holes in the PbO matrix are exactly above and below these units (Figure 1b).

The lead oxide $[\text{O}_{22}\text{Pb}_{30}]^{16+}$ block in the structure of **1** is remarkable in its exceptional topological complexity, which has no analogues among the known PbO derivatives.¹⁰ⁿ It consists of 22 symmetrically independent OPb_4 tetrahedra that, in addition, play different roles in the topological organization of the layer. To discuss the topology of the tetrahedral layer in more detail, we shall use the approach first suggested in ref 10n. A single OPb_4 tetrahedron is symbolized by a square. Thus, the $[\text{OPb}]$ layer in tetragonal PbO corresponds to a 2D layer of black squares that fill the plane without gaps and overlaps. In turn, tetrahedral layers in the PbO derivative structures correspond to 2D arrangements of black and white squares, where the latter symbolize vacancies. Figure 2a shows the 2D array of squares that represents the arrangement of OPb_4 tetrahedra within the $[\text{O}_{22}\text{Pb}_{30}]^{16+}$ block in the structure of **1**. Each black square is labeled by a number that corresponds to the designation of the O site at the center of the OPb_4 tetrahedron. The topological function of a tetrahedron within the layer can be visualized by investigation of the local coordination of a

- (9) Crystallographic data for $\text{Pb}_{31}\text{O}_{22}\text{Br}_{10}\text{Cl}_8$ (**1**): triclinic, $P\bar{1}$, $a = 12.1192(7) \text{ \AA}$, $b = 16.2489(10) \text{ \AA}$, $c = 18.3007(11) \text{ \AA}$, $\alpha = 93.104(2)^\circ$, $\beta = 95.809(2)^\circ$, $\gamma = 111.252(1)^\circ$, $V = 3325.4(3) \text{ \AA}^3$, $Z = 2$; crystal dimensions $0.10 \times 0.08 \times 0.001$; $\rho_{\text{calcd}} = 7.85 \text{ g cm}^{-3}$, $\mu = 84.502 \text{ mm}^{-1}$. Data collection: Bruker SMART APEX CCD diffractometer, 33 290 total reflections, 21 894 unique reflections, 8416 unique reflections, $|F_o| \geq 4\sigma F_o$. The structure solved by direct methods and refined to $R1 = 0.066$, $wR2 = 0.121$, and $S = 0.798$ (anisotropic displacement parameters for Pb, Br, and Cl atoms). Semiquantitative electron microprobe analysis provided the Br/Cl ratio as 12:6, which is close to that determined by structural analysis, taking into account the high volatility of Cl under an electron beam.
- (10) (a) Keller, H. L. *Z. Anorg. Allg. Chem.* **1982**, *491*, 191–198. (b) Behm, H. *Acta Crystallogr.* **1983**, *C39*, 1317–1319. (c) Mentzen, B. F.; Latrach, A.; Bouix, J.; Boher, P.; Garnier, P. *Mater. Res. Bull.* **1984**, *19*, 925–934. (d) Latrach, A.; Mentzen, B. F.; Bouix, J. *Mater. Res. Bull.* **1985**, *20*, 853–861. (e) Riebe, H.-J.; Keller, H. L. *Z. Anorg. Allg. Chem.* **1988**, *566*, 62–70. (f) Langecker, C.; Keller, H. L. *Z. Anorg. Allg. Chem.* **1994**, *620*, 1229–1233. (g) Vassilev, P.; Nihitjanova, D. *Acta Crystallogr.* **1998**, *C54*, 1062–1068. (h) Yeom, Y. H.; Kim, Y.; Seff, K. *J. Phys. Chem.* **1997**, *B101*, 5314–5318. (i) Li, Y.; Krivovichev, S. V.; Burns, P. C. *J. Solid State Chem.* **2000**, *153*, 365–370. (j) Li, Y.; Krivovichev, S. V.; Burns, P. C. *J. Solid State Chem.* **2001**, *158*, 74–77. (k) Krivovichev, S. V.; Li, Y.; Burns, P. C. *J. Solid State Chem.* **2001**, *158*, 78–81. (l) Krivovichev, S. V.; Burns, P. C. *Z. Kristallogr.* **2002**, *217*, 451–459. (m) Krivovichev, S. V.; Burns, P. C. *Z. Kristallogr.* **2003**, *218*, 357–365. (n) Krivovichev, S. V.; Armbruster, T.; Depmeier, W. *J. Solid State Chem.* **2004**, *177*, 1321–1332. (o) Krivovichev, S. V.; Avdontseva, E. Yu.; Burns, P. C. *Z. Anorg. Allg. Chem.* **2004**, *630*, 558–562.
- (11) Bonhomme, F.; Alam, T. M.; Celestian, A. J.; Tallant, D. R.; Boyle, T. J.; Cherry, B. R.; Tissot, R. G.; Rodriguez, M. A.; Parise, J. B.; Nyman, M. *Inorg. Chem.* **2005**, *44*, 7394–7402.

- (12) O'Keefe, M.; Hyde, B. G. *Crystal Structures. I. Patterns and Symmetry*. Mineralogical Society of America Monograph: Washington, DC, 1996.
- (13) (a) Carré, D.; Guittard, M.; Jaulmes, S.; Mazurier, A.; Palazzi, M.; Pardo, M. P.; Laurelle, P.; Flahaut, J. *J. Solid State Chem.* **1984**, *55*, 287–292. (b) Quebe, P.; Terbüchte, L. J.; Jeitschko, W. *J. Alloys Compd.* **2000**, *302*, 70–74. (c) Cario, L.; Kabbour, H.; Meerschaut, A. *Chem. Mater.* **2005**, *17*, 234–236. (d) Kabbour, H.; Cario, L.; Danot, M.; Meerschaut, A. *Inorg. Chem.* **2006**, *45*, 917–922.
- (14) Liao, J.-H.; Kanatzidis, M. G. *Chem. Mater.* **1993**, *5*, 1561–1569.
- (15) (a) Johnson, V.; Jeitschko, W. *J. Solid State Chem.* **1974**, *11*, 161–166. (b) Bobev, S.; Sevov, S. C. *Inorg. Chem.* **1999**, *38*, 2672–2676.

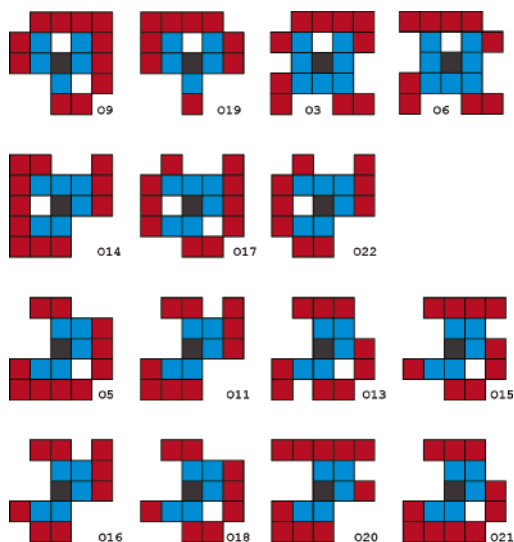


Figure 3. Local coordinations of OPb_4 tetrahedra within the $[\text{O}_{22}\text{Pb}_{30}]^{16+}$ 2D layer in the structure of **1**. Central tetrahedra are shown in gray, first coronas in blue, and second coronas in red.

given square by the adjacent squares, i.e., by all squares with which it has common points. The arrangement of black squares around the central square is designated the first corona,¹⁶ and we denote it as $c^1(p)$, where p is a square number. In turn, the second corona, $c^2(p)$, is defined as a set of black squares that surround the first corona, and so on.

Figure 2b provides the schemes of first coronas for all of the 22 tetrahedra present in the $[\text{O}_{22}\text{Pb}_{30}]^{16+}$ blocks. There are some coronas that are common for several tetrahedra. For instance, the O1Pb_4 , O7Pb_4 , O8Pb_4 , and O10Pb_4 tetrahedra have the same coronas consisting of six tetrahedra arranged around the central one in the same way. To further investigate whether topological functions of the tetrahedra are different, one has to examine their second coronas. Figure 3 demonstrates that, despite the fact that the first coronas of some tetrahedra are identical, their second coronas are different, and therefore the topological functions of the tetrahedra are different. For instance, the O9Pb_4 and O19Pb_4 tetrahedra have identical first, but different second, coronas. The tetrahedra centered by the O5, O11, O13, O15, O16, O18, O20, and O21 atoms are distinguished by their second coronas, whereas their first coronas are the same (Figure 3).

The situation is more complicated for the O1Pb_4 and O8Pb_4 tetrahedra because they have identical first and second coronas (Figure 4). However, their third coronas are different, and therefore their topological functions within the sheet are inequivalent. To our knowledge, this is the first example of a structure where third coronas are necessary to reveal topological differences between single tetrahedra.

(16) Krivovichev, S. V.; Filatov, S. K.; Semenova, T. F. Z. *Kristallogr.* **1997**, *212*, 411–417.

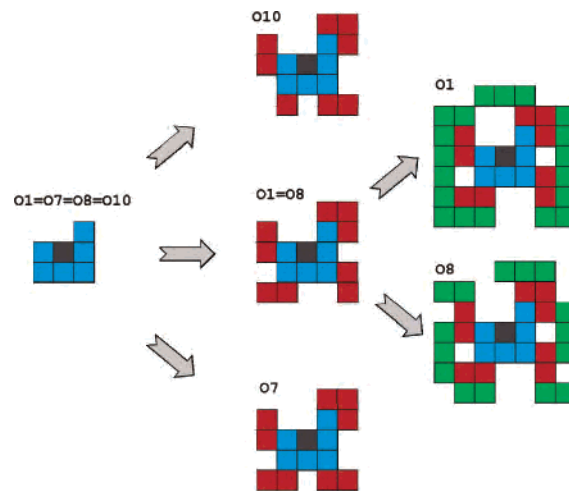


Figure 4. Description of the topology of the $[\text{O}_{22}\text{Pb}_{30}]^{16+}$ 2D layer in the structure of **1**. OPb_4 tetrahedra centered by the O1, O7, O8, and O10 atoms have the same first coronas (shown in blue). The second coronas (shown in red) are different for the O10- and O7-centered tetrahedra; however, they are the same for the O1Pb_4 and O8Pb_4 tetrahedra. The O1Pb_4 and O8Pb_4 tetrahedra have different third coronas (shown in green). See the text for details.

All 22 symmetrically independent tetrahedra in the $[\text{O}_{22}\text{Pb}_{30}]^{16+}$ block have unique functions in the topology of this unit. This topological complexity is exceptional and, as far as we know, has not been observed in any ordered tetrahedral structure. From the chemical viewpoint, the appearance of such complexity should be ascribed to the incorporation of octahedral halide clusters into the metal oxide matrix that induces modification of the latter in a complex way. However, the model of black and white squares proposed to describe this level of complexity is rather simple. In particular, it is especially suitable for modeling self-organization of complex topologies using cellular automata that have attracted much attention within the past few years.¹⁷

Acknowledgment. This work was financially supported by the Russian Ministry of Science and Education (Grant RNP 2.1.1.3077) and through a DFG–RFBR collaborative grant (Grant 06-05-04000-NNIO_a).

Supporting Information Available: X-ray crystallographic data in CIF format and a list of Pb–O and Pb–X bond lengths and bond valence sums incident upon Pb sites. This material is available free of charge via the Internet at <http://pubs.acs.org>.

IC060166M

(17) (a) Ilachinski, A. *Cellular Automata: a Discrete Universe*; World Scientific: London, 2001. (b) Krantz, S. G. *Bull. Am. Math. Soc.* **2002**, *40*, 143–150. (c) Wolfram, S. *A New Kind of Science*; Wolfram Media, Inc.: Champaign, IL, 2002. (d) Krivovichev, S. V. *Acta Crystallogr.* **2004**, *A60*, 257–262.